Optical phonons in R_2BaMO_5 oxides with M = Co, Ni, Cu, and R = a rare earth

A. de Andrés, S. Taboada, and J. L. Martínez
Instituto de Ciencia de Materiales de Madrid, Consejo Superior de Investigaciones Científicas, Facultad de Ciencias, C-4, Universidad Autónoma de Madrid, Madrid, E-28049, Spain

A. Salinas, J. Hernández, and R. Sáez-Puche
Departamento Química Inorgánica, Facultad Ciencias Químicas, Universidad Complutense de Madrid, E-28040, Spain
(Received 25 January 1993)

Compounds with the formula R_2BaMO_5 where R = rare earth and M = Co, Ni, or Cu, have been studied with Raman spectroscopy. The lattice dynamics of the three different crystallographic phases adopted by these systems (space groups *Immm*, *Pnma*, and *P4/mbm*) is discussed in relation to the transition-metal–oxygen coordination, and to the binding M-O and R-O distances. An almost complete identification of the normal modes has been performed for the compounds with the *P4/mbm* structure and an estimation of the parameters of the M-O and R-O stretching force constants has been obtained for the *Immm* and *P4/mbm* structures.

I. INTRODUCTION

Oxides with the formula R_2BaMO_5, where R = rare earth, and M = Co, Ni, or Cu, present three different crystallographic structures depending on the transition metal and the size of the R ion. Nickel oxides, with R = Nd to Yb, have been recently structurally described as belonging to the *Immm* space group,[1,2] this structure is also adopted by some Co oxides. By contrast, most of the cuprates show a much more complicated structure with the *Pnma* space group and contains four formulas in the primitive cell.[3] Nickelates with the smallest rare-earth ions (Tm, Yb, and Lu) can also be synthetized in this later orthorhombic structure.[4] Some of the compounds, actually cuprates with La and Nd, which are the lanthanide ions with larger ionic radii, present a tetragonal *P4/mbm* (Ref. 5) structure, which contains two formulas in the primitive cell. The transition-metal environments and their stacking are different from one structure to the other giving rise to different magnetic and transport properties.

The *Immm* structure consists of one-dimensional (1D) chains of M-O octahedra (Fig. 1) connected by the apical oxygens [called O(2)] along the a axis. The octahedra are flattened with M-O(2) distances surprisingly short (around 1.88 Å) which are very unusual bond distances for Cu and Ni oxides. The peculiarities of this structure, together with the distortion of the octahedra give rise to Y_2BaNiO_5 to 1D antiferromagnetic (AF) fluctuations along the Ni-O(2) chains.[6] When the diamagnetic Y is substituted by a different paramagnetic rare earth (Nd-Tm), both sublattices become 3D-AF ordered at temperatures as high as 40 K.[7] The optical Raman phonons have been studied in nickelates with this structure and an evaluation of the force constants was obtained.[8] These compounds present Raman spectra which agree with the group theory predictions but a weak forbidden Raman peak; the infrared (IR) active stretching mode of the apical oxygen, is observed in the Raman spectra because of the presence of some defects, for example, small quantities of other rare earth.

In the *Pnma* structure the M ions are surrounded by five oxygens forming isolated square pyramids (Fig. 1) [the apical oxygens are called O(3)]. This phase, in the case of the cuprates, is very often found as an impurity in the superconductor $YBa_2Cu_3O_{6+x}$ synthesis and is now being used as a pinning center inside the superconducting matrix in order to increase the critical current. An in-

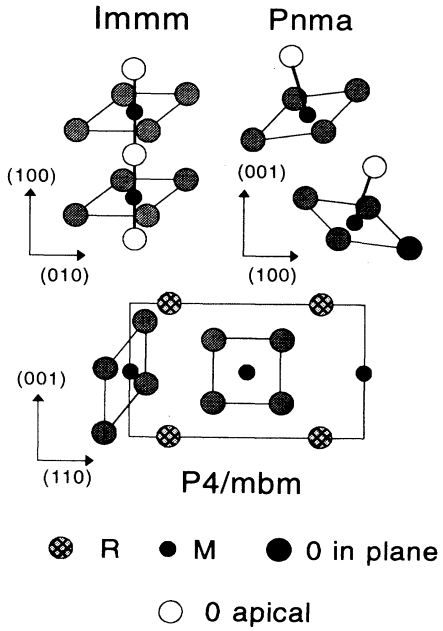

FIG. 1. Metal environments in the three studied structures: *Immm* with oxygen octahedra (*C*-6) around the 3*d* metal, *Pnma* with pyramids (*C*-5), and *P4/mbm* with square planes (*C*-4) for compounds with R_2BaMO_5 formula.

teresting property is the dimorphism of the Lu, Yb, and Tm nickelates which can be obtained in both structures (*Immm* or *Pnma*). In this later compound, there is not 3D-AF until 1.5 K for the *Pnma* structure, while 3D-AF ordering of the Ni and R sublattices is observed for the *Immm* phase (T_N=40 K).[4] The comparison of the optic phonons and magnetic properties of the Tm_2BaNiO_5 compound in both structures is given in Ref. 9. From a structural point of view, the difference between cuprates and nickelates consists only in the more irregular oxygen pyramids in the Cu compounds. Recently, a careful Raman study of cuprates with this structure and an assignment of the normal modes has been reported.[10]

The oxygen coordination of the transition metal in the *P4/mbm* structure is four, forming planar squares around the metal (Fig. 1), which are not connected to each other and are present in two perpendicular planes parallel to the *c* axis. To our knowledge no study of the optical phonons has been performed in these compounds.

The study of lattice dynamics of this type of oxides is important by itself and by their relation with similar high T_c superconductor oxides. These materials usually have nonsuperconductor parent compounds which share most of the structural and dynamical properties. The bond strength between ion pairs are comparable and sometimes transferable quantities between these compounds and the related but little known high-T_c compounds.

Several studies on the lattice dynamics in related systems reflect the high complexity caused by the huge variety of new compounds that can be obtained with different stoichiometry and structure, and as a consequence with different physical properties (magnetic order, electronic structure, superconducting states, etc.).[11–13]

II. EXPERIMENTAL DETAILS

The different R_2BaMO_5 oxides were prepared as policrystalline samples mixing the stoichiometric amounts of the high-purity oxides, R_2O_3 (99.999%), NiO (99.99%), CuO (99.999%), and $BaCO_3$ (99.999%). The homogenized mixture was heated in air at 950 °C for 12 h, then it was regrounded and reheated at 1050 °C for another 12 h. In the case of the nickelates, a third thermal treatment at 1200 °C was necessary to obtain these oxides as pure phases.

The cobalt samples were obtained following the same treatment described before, but they were obtained in an argon flow due to the high instability of Co^{+2} in air at the high temperatures necessary to prepare these compounds. The x-ray-diffraction data shown that all the samples are single phases and present the *Immm*, *Pnma*, or *P4/mbm* structures.

Raman-scattering experiments have been performed with an *X-Y* Dilor multichannel spectrometer using a spectra physics Ar^+ laser as excitation source. The spectra were recorded at temperatures between 300 and 4.2 K in the backscattering geometry using a continuous flux Oxford Instrument cryostat. The beam power on the sample was less than 20 mW in order to avoid possible surface damage due to the sample heating. All the spectra have been corrected by the spectral response of the experimental setup.

III. RESULTS AND DISCUSSION

A. Normal mode analysis

Both space groups, *Immm* and *Pnma*, are orthorhombic with the D_{2h} point group, but with a different number of formulas in the primitive cell (Z=1 and 4, respectively). For that reason, the number of active normal modes is very different for the two structures. The factor group analysis of the *Immm* structure[8] shows that, out of the 27 normal modes, 9 even modes are Raman active and 14 odd modes are infrared active. The irreducible representations of the active optical modes $\mathbf{k}=\mathbf{0}$ are

$$3A_g+1B_{1g}+2B_{2g}+3B_{3g}+5B_{1u}+5B_{2u}+4B_{3u}\ .$$

In this highly symmetric structure the *M*, O(2), and Ba ions are located at inversion centers, so they do not contribute to any Raman mode. Three of the Raman active modes correspond to *R* ion motions and the remaining six correspond to the oxygens O(1), which form the basal planes of the Ni-O octahedra. The apical oxygens O(2) catenate the successive octahedra and contribute only to infrared modes. The atomic displacements of the Raman active oxygen normal modes together with one IR mode are shown in Fig. 2.

The phase with the *Pnma* space group has a large primitive cell with 36 ions and 108 normal modes of vibration. The number of Raman active modes is 52 and that of IR modes is 35. In this case all the ions can contribute to the Raman modes. Abrashev and Iliev[10] have

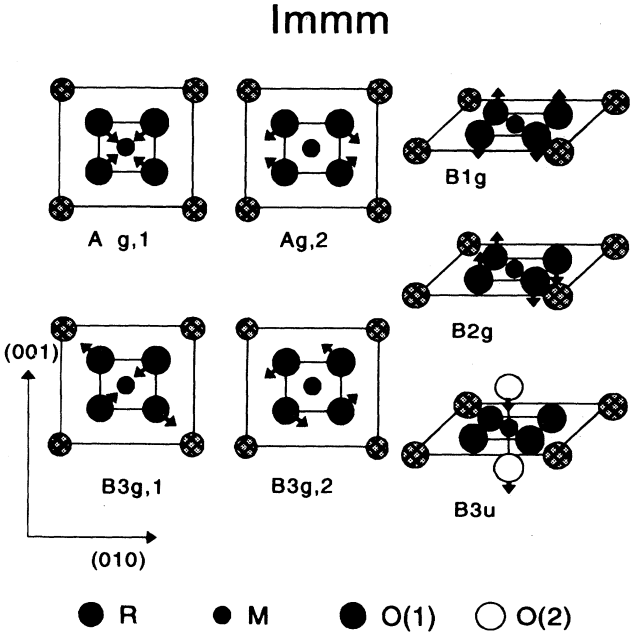

FIG. 2. Description of the Raman active modes of the in-plane oxygen ions in the *Immm* structure, and one IR mode of the apical oxygen.

done a careful assignation of the observed Raman peaks which will be commented on later.

The tetragonal phase *P4/mbm* has the D_{4h} point group and, as in the *Immm* structure, only *R* ions and one type of oxygen [called O(1)], which are those forming the squares around the metal *M*, are not at inversion centers and so participate in the Raman active phonons. This structure contains planes with *M*, O(1), and *R* ions, which are (110) and ($\bar{1}$10) planes parallel to the *z* axis, nearly identical to the (001) *xy* planes in the *Immm* structure. In fact, the vibrational modes are very similar in the two structures. The number of Raman active normal modes given by the factor group analysis is 11, and 17 odd modes are infrared active. The irreducible representations of the active modes at $\mathbf{k}=\mathbf{0}$ is

$$3A_{1g}+2B_{1g}+3B_{2g}+3E_g+6A_{2u}+11E_u \ .$$

Among the Raman modes, seven are associated with oxygen vibrations ($2A_g+1B_{1g}+2B_{2g}+2E_g$) and four are associated with *R* motions ($1A_g+1B_{1g}+1B_{2g}+1E_g$). Because the primitive cell contains two formulas ($Z=2$), there are two equivalent sets of metal *M* surrounded by four oxygens; the structure therefore presents phonons which differ only in the phase of the vibration of one set with respect to the other. Actually, A_{1g} and B_{2g} modes are in-phase and out-of-phase phonons of the same vibration. These two squares of oxygen ions around the *M* ions are practically independent because they do not share any ion so it is expected that the frequencies of these phonons (in and out of phase) will be very similar or even indistinguishable experimentally. In that way, only five O peaks and three *R* peaks are expected. In Fig. 3, A_{1g}, B_{1g}, and E_g modes of one of the two "squares" are shown; the B_{2g} modes are not shown. The similarities between these and the *Immm* phase modes can be easily seen.

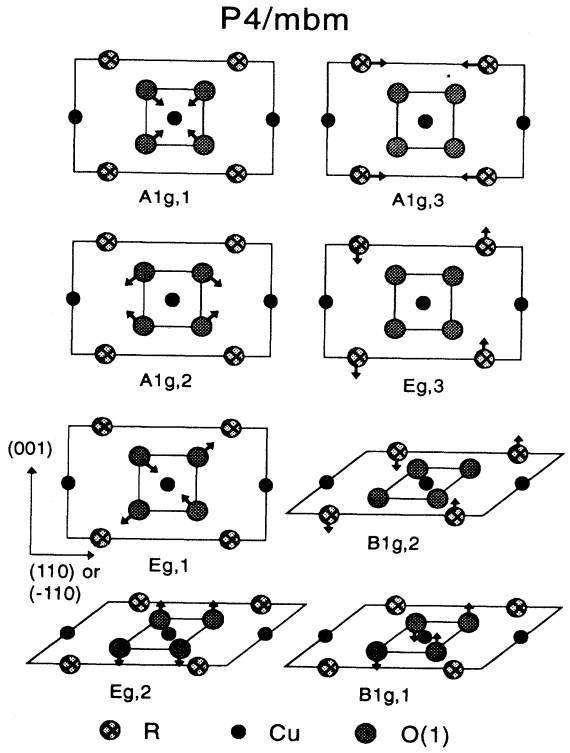

FIG. 3. Description of the Raman active modes of the *P4/mbm* structure. The B_{2g} modes are not shown: they are the same as A_{1g} ones but the two equivalent units [in planes parallel to the (110) and ($\bar{1}$,1,0) directions] vibrating in opposition of phase.

B. Lattice vibrations

Figure 4 shows characteristic Raman spectra for compounds belonging to the three different structures. The upper part corresponds to compounds with the *Immm* structure, the sharpest peaks at low frequencies are due to (*R*) rare-earth ion motions and the others to the in-plane oxygens. In the spectra of Fig. 4(iii), the phonons of the less symmetric phase (*Pnma*) are shown. The highest-energy phonons can probably be assigned to stretching oxygen modes while, in the lower-frequency region, more than one kind of ion participates in the normal modes. A remarkable feature is the big difference in the intensity of some oxygen modes (marked with an asterisk in the figure) in the spectra of the two compounds. This change can only be caused by the change in the transition metal (Ni to Cu) because the structure is the same and the interatomic distances are very similar. Finally, Fig. 4(ii) shows the Raman phonons of the Nd and La cuprates (the intensity has been corrected by the incident power). Note that these spectra are similar to the *Immm* phase in number and frequency of the peaks but not in their relative intensities.

1. Immm phase: Sixfold metal coordination (C-6)

In the *Immm* compounds, the very different atomic masses of the yttrium and the rare-earth ions gave us the possibility to observe a very clear frequency shift of the first two peaks, and only in these two modes, which demonstrates that they effectively correspond to phonons which actually involve only *R* ion movements.[8] The remaining modes are then only related with oxygen motions. The highest allowed Raman mode corresponds to the stretching of the in-plane oxygen ions and appears in all these compounds between 500 and 540 cm^{-1}. The peak observed around 730 cm^{-1} as a weak shoulder in all the studied nickelates[9] is the most important peak in the spectrum of Eu_2BaCoO_5 [marked with an arrow in Fig. 4(a)]. We assign this peak to the B_{3u} infrared *M*-O(2) stretching mode (forbidden in Raman scattering and shown in Fig. 2), which appears with a very strong oscillator force in the IR spectrum[9] at 786 cm^{-1} in the Tm_2BaNiO_5 compound. The *M*-O(2) distance is very short (around 1.88 Å), so the frequency is expected to be the highest of the normal modes.

The very large intensity of the Raman forbidden 706 cm^{-1} peak in the Eu compound can probably be produced by some kind of disorder in the structure. The presence of different rare-earth ions as an impurity would break the inversion symmetry of the apical oxygens and

transform this mode in a Raman allowed one. The other possibility is that the structure is not actually correctly described by the *Immm* group but by some less symmetric group or that some kind of local distortion is present. We are more inclined to favor the first explanation because of the x-ray-diffraction analysis and also because the number and frequencies of the Raman peaks correspond to the expected ones for the *Immm* phase. Another possibility, which is not exclusive with the previous one, is that the incident or scattered energies can be in resonance with some electronic transition which induces, through electron-phonon Fröhlich interaction, the Raman activity for the LO odd phonons. More experimental work is now in progress in order to shed some light on the different possibilities.

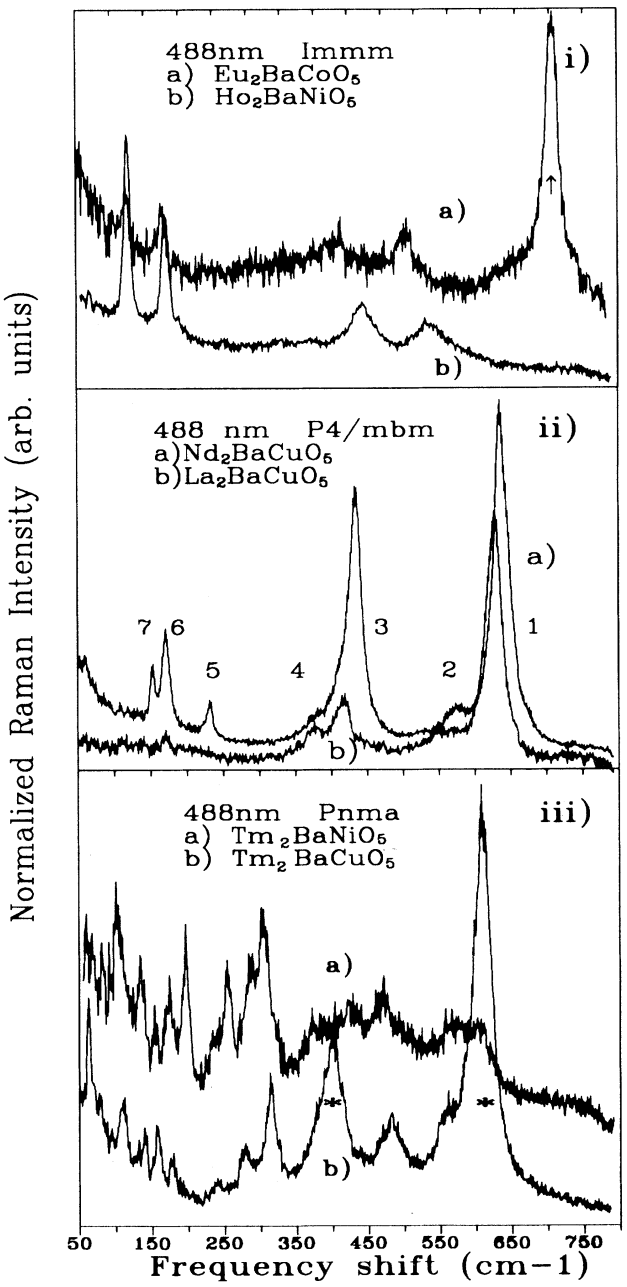

FIG. 4. Raman spectra at 300 K of several compounds in the three structures: (i) *Immm*, (ii) *P4/mbm*, and (iii) *Pnma*. In each part, the spectra have been shifted vertically for an easier sight. Symbols are explained in the text.

2. *P4/mbm phase: Fourfold metal coordination (C-4)*

Seven peaks are clearly seen in the Nd_2BaCuO_5 spectra compared to the eight expected ones. Following the previous discussion on the frequency degeneracy of the A_{1g} and B_{2g} phonons, only 8 different peaks are expected instead of 15. By comparison to the *Immm* spectra, where it has been settled that the lowest-energy peaks correspond to the R ion motions, it can be said that the rare-earth modes in this structure are those numbered in Fig. 4(b) as "5, 6, and 7." The low intensity of these modes in La compounds must be related to the characteristics of this particular ion. The peaks at higher energy are oxygen modes. The assignation of the observed peaks to the normal modes is summarized in Table I, together with the *Immm* modes of the cobalt compound and some nickelates.

Because the stretching modes of the *Immm* (A_g and B_{3g}) and *P4/mbm* (A_{1g} and E_g) structures consist of the same pattern of atomic displacements, they can be directly compared. In these compounds, the rare-earth ions play an important role in the determination of the frequency of the phonons, especially for the symmetric and antisymmetric stretching modes which are the highest-energy ones, because the M-O(1) and R-O(1) distances are very similar and the three ions are collinear (in the *Immm* phase) or nearly collinear (in the *P4/mbm* phase). That is the reason why both distances must be considered in order to compare the frequencies in different compounds or structures, even in a first approximation. In fact, fixing a $3d$ metal, the M-O distance is nearly invariant and the R-O distance has the largest variation, which is responsible for the changes in the frequency.

A useful phenomenological expression for the stretching force constants between ions i and j (Ref. 14) is

$$F_{ij}=K_1E_iE_j/d_{ij}^3+K_2 ,$$

where E_i and E_j are the electronegativities of the ions i and j, d_{ij} is the interatomic distance, and K_1 and K_2 are constants. The frequencies of the oxygen stretching phonons, which are the simplest normal modes because they have nonimportant contributions from angle-bending force constants, are well described with this model. For example, the A_g (of the *Immm* structure) and A_{1g} (of the *P4/mbm* structure) phonons have frequencies equal to

$$\Omega_{\rm sym}=[(F_{\text{O-}M}+F_{\text{O-}R}+2f_{rr}+f'_{rr})/M_{\rm O}]^{1/2} ,$$

where f_{rr} and f'_{rr} are related to the interaction between two perpendicular and collinear bonds, respectively, and $M_{\rm O}$ is the oxygen mass. The frequency of the antisymmetric stretching mode (B_{3g} for *Immm* and E_g for *P4/mbm*) is described by

TABLE I. Observed frequencies (in cm^{-1}) and mode assignment for the *Immm* and *P4/mbm* structures; the lower part summarizes the relevant interatomic distances.

	R_2BaMO_5							
	Immm					*P4/mbm*		
Ion involved/	Co			Ni			Cu	Normal
Normal mode	Eu	Y	Ho	Er	Tm	La	Nd	mode
		115						
R/B_{3g}	115	163	118	118	115	157	152	B_{1g},1 or E_g,2
R/A_g	165	230	171	171	170	170	170	A_{1g},3+B_{2g},3
O/B_{1g},		267	236	228			231	B_{1g},1 or
B_{2g} or B_{3g},2	302	331		309	327	376	380	E_g,2
O/A_g, 2	342	374	375	387	389	412	431	A_{1g},2+B_{2g},2
O/B_{3g},1	410	440	444	450	458	550	572	E_g,1
O/A_g,1	507	535	539	539	550	624	635	A_{1g},1+B_{2g},1
O/B_{3u}	709		740	740	740			
Distances (Å)								
M-O in plane	2.222	2.182	2.185	2.183	2.176	1.93	1.931	
M-O apical	1.888	1.881	1.882	1.874	1.876			
R-O in plane	2.313	2.250	2.248	2.229	2.221	2.325	2.384	

$$\Omega_{\text{asym}}=[(F_{\text{O-}M}+F_{\text{O-}R}-2f_{rr}+f'_{rr})/M_{\text{O}}]^{1/2} .$$

Using the previous expression for the force constants we have

$$\Omega^2_{\text{sym}}=C_1[K_1E_{\text{O}}E_R(E_M/E_Rd^3_{M\text{-O}}+1/d^3_{R\text{-O}})+C_2]$$

and the same expression is valid for Ω^2_{asym} with a different value of the constant C_2. Representing the square of the frequency versus the function of the distances in parenthesis, a linear behavior is expected with the same slope for the symmetric and antisymmetric stretching modes if the interaction constants f_{rr} and f'_{rr} are similar for all these compounds. This condition is quite satisfied at least for the nickelates.[8]

Figure 5 summarizes the square of the observed frequencies for the oxygen modes in all measured compounds with these two structures versus the previously defined function of the transition metal *M* to in-plane oxygen and the oxygen to rare-earth distances. A linear dependence, of the two stretching and two bending oxygen modes, is observed on the defined variable. The slopes for the stretching modes are nearly equal, as expected, but different to those of the bending modes which are related to angle bending force constants of lower value. The goodness of the fit for the four modes indicates that the frequencies have no large dependence on the overall structure. This would mean that, in a first approximation, the *M* in-plane oxygen force constants are not affected by the presence of 1 or 2 apical oxygens or by changing the transition-metal ion. Such a simple approach, which summarizes the electronic characteristics of the atoms by their polarizability constant, seems to correctly explain the dependence of the phonon frequencies. From the slopes it is possible to obtain the value of K_1 and from the difference in the ordinates, between the lines representing the symmetric and antisymmetric stretching modes, we obtain the value of f_{rr}. In that way these constants ($K_1=4.66$ mdyne Å^2 and $f_{rr}=0.306$ mdyne/Å) are some kind of averaged values for all the compounds in the plot.

3. *Pnma phase: Fivefold metal coordination (C-5)*

Looking at the complicate *Pnma* spectra, note that the upper limit for phonons is around 616 cm^{-1}. The differences in the maximum frequencies in the three structures are related to differences in the *M*-O distances: around 2.2 Å in the *Immm* phases and 1.93 Å in the *P4/mbm* one. In nickelates, the *Pnma* structure presents three very similar Ni-O distances around 2 Å [Ni-O(3): 1.996, Ni-O(1); 2.016 and Ni-O(2); 2.066 Å for the Tm compound[4]], while in cuprates there are two groups of

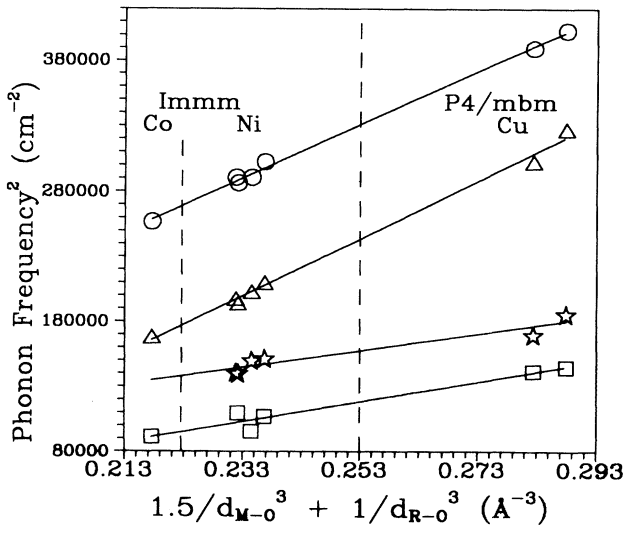

FIG. 5. Square of the oxygen mode frequencies vs a function of metal-oxygen and rare-earth–oxygen distances for Co, Ni, and Cu oxides with the *Immm* or *P4/mbm* structures. The lines are the least-square fits of the experimental points.

distances; one around 2.2 Å [Cu-O(3): 2.206 Å in the Tm compound] and the other around 2 Å [Cu-O(1): 1.975 Å; Cu-O(2): 2.015 Å in the Tm compound] related to the differences in the bonds formed by the Ni and Cu ions.

We have approached this problem differently than Abrashev and Iliev. These authors have performed a very careful analysis of their spectra considering the displacements in the three directions of the crystallographic axis of all different type of atoms. The main problem is that they need to consider that each normal mode is due to only one type of atom and do not take into account that some bonds are tighter than others and require a more molecular viewpoint, at least for the M-O units (squares, pyramids, and octahedra).

In order to study the highest-energy phonons, which are very probably oxygen modes, we will start from the normal modes of a tetragonal pyramidal ZXY_4 molecule[15] (the correspondence is X=transition metal, Y=in-plane oxygen, and Z=apical oxygen). This molecule presents nine normal modes: ν_1 is the stretching of the X-Z bond, ν_2 is the symmetric stretching of the four X-Y bonds, ν_4 is the antisymmetric stretching mode, and the other modes are bending and tilting vibrations. In molecules, the ν_1 mode is usually the highest-frequency one but, in this case, we think that the vibration ν_2 [which is the in-phase stretching mode of the in-plane O(1) and O(2) ions] corresponds to the 616 cm^{-1} peak, which is the highest-energy one. In the cuprates, the apical oxygen O(3) is at considerably larger distance (around 2.2 Å) than the in-plane oxygens [O(1) and O(2)] which are around 2 Å. Looking at the environments of the three different oxygen ions we can observe that O(1) and O(2) are identical except for small variations in the distances, the first neighbors (at distances below 3 Å) are 1 Cu, 1 R nearly collinear [Cu-O(2,3)-R], 2 R, 2 O(2,3), and 2 Ba. The O(3) ion has no collinear bonds or other near oxygen ions. The distances and kind of bonds of the oxygen ions indicate that O(3) is less tightly bound than the O(1) and O(2). It is then more probable that the 616 cm^{-1} peak corresponds to the O(1,2) oxygens. Plotting the frequencies of the highest mode for all studied compounds versus the relevant M-O distance (see Fig. 6), we again obtain a correct behavior when the chosen distance for the *Pnma* structure is the M-O(1,2) one. The expected frequency for a 2.2 Å distance will be around 540 cm^{-1}, note that a peak at 555 cm^{-1} is observed, nevertheless, the number of possible modes is too high (30 oxygen modes are expected) to make any reliable assignation.

Comparing the spectra from Cu and Ni isomorphic compounds, a clear difference in the intensity of two peaks is observed. The Raman efficiency, at a given temperature, is related to the amplitude of the modulation of the dielectric function, i.e., to the optical absorption, at the laser frequency.[16] Looking at all the spectra of the studied compounds (some of them are plotted in Fig. 4) we observe that the cuprates always present a higher intensity of the in plane oxygen modes, relative to the other modes, than nickelates. This may indicate that in cuprates there is an electronic transition in the Cu in-plane oxygen at energies around 2.5 eV which is not present in nickelates. Studies of the dependence of the intensity with the incident wavelength are planed in order to check if these modes are resonant at different wavelengths for nickelates and cuprates.

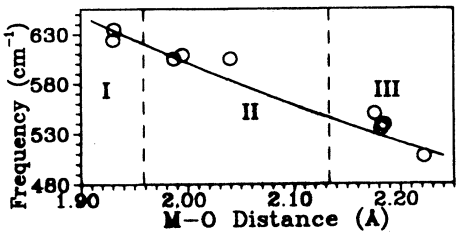

FIG. 6. Oxygen stretching mode frequency vs 3d metal to oxygen distance for the three structures: region I corresponds to *P4/mbm* Cu oxydes, region II to *Pnma* Cu and Ni oxides and region III to *Immm* Ni and Co oxydes. The solid line is a fit of the experimental frequencies with a form: $y = Ax^{-3/2}$ with $A = 1700\ cm^{-1}$.

IV. CONCLUSIONS

Raman active phonons of R_2BaMO_5 compounds in three of their structures have been observed and identified. In nickelates with the *Immm* structure, a weak peak corresponding to an IR active and Raman forbidden mode is seen because of the presence of lattice defects. In the Eu_2BaCoO_5 compound this IR mode is enhanced probably because of some electronic resonance with the incident wavelength. The parameters for stretching force constants of M-O and R-O bonds have been obtained for the compounds with *Immm* and *P4/mbm* structures. The frequencies of the in-plane oxygen stretching mode are correctly explained with the same force constants for the three structures, which means that they are not affected by the presence of one or two apical oxygens nor are they directly affected by the metal M but only through the distances. The intensity of the oxygen peaks is clearly related to the 3d metal, which is the important ion relative to the differences in the electronic structures and, therefore, in the resonant conditions of the experiments.

ACKNOWLEDGMENTS

We acknowledge financial support from the Comisión Interministerial de Ciencia y Technología (Ministerio de Educación y Ciencia) under Contract No. MAT 91-0588. A. de A. thanks the Ministerio de Asuntos Exteriores and the Grupo Especializado de Física del Estado Sólido for travel support.

[1]S. Schiffer and H. K. Müller-Bushbaum, Z. Anorg. Allg. Chem. **532**, 10 (1986).

[2]J. Amador, E. Gutiérrez-Puebla, M. A. Monge, I. Rasines, C. Ruiz-Valero, F. Fernández, R. Sáez-Puche, and J. A. Campa, Phys. Rev. B **42**, 7918 (1990).

[3]A. Salinas-Sánchez, J. L. García-Muñoz, J. Rodríguez-Carvajal, R. Sáez-Puche, and J. L. Martínez, J. Solid State Chem. **100**, 201 (1992).

[4]A. Salinas-Sánchez, R. Sáez-Puche, J. Rodríguez-Carvajal, and J. L. Martínez, Solid State Commun. **78**, 481 (1991); E. García-Matres, J. L. Martínez, J. Rodríguez-Carvajal, J. A. Alonso, A. Salinas-Sánchez, and R. Saez-Puche, J. Solid State Chem. (to be published).

[5]A. Salinas-Sánchez and R. Sáez-Puche, Solid State Ionics. See also T. Mochiku *et al.*, J. Phys. Soc. Jpn. **60**, 1959 (1991).

[6]R. Sáez-Puche, J. M. Coronado, C. L. Otero Díaz, and J. M. Martin Lorente, J. Solid State Chem. **93**, 461 (1991).

[7]G. G. Chepurko, Z. A. Kazei, D. A. Kudrjavtsev, R. Z. Levitin, B. V. Mill, N. Popova, and V. V. Snegirev, Phys. Lett. A **157**, 81 (1991). See also J. A. Alonso, J. Amador, J. L. Martínez, I. Rasines, J. Rodríguez-Carvajal, and R. Sáez-Puche, Solid State Commun. **76**, 467 (1990).

[8]A. de Andrés, J. L. Martínez, R. Sáez-Puche, and A. Salinas-Sánchez, Solid State Commun. **81**, 931 (1992).

[9]A. Salinas-Sánchez, R. Sáez-Puche, F. Fernández, A. de Andrés, A. E. Lavat, and E. J. Barán, J. Solid State Chem. **99**, 63 (1992).

[10]M. V. Abrashev and M. N. Iliev, Phys. Rev. B **45**, 8046 (1992).

[11]M. K. Crawford, G. Burns, and F. Holtzberg, Solid State Commun. **70**, 557 (1989).

[12]G. Burns, F. H. Dacol, C. Feild, and F. Holtzberg, Solid State Commun. **77**, 367 (1991).

[13]L. A. Farrow, R. Ramesh, and J. M. Tarascon, Phys. Rev. B **43**, 418 (1991).

[14]J. E. Eldridge and F. E. Bates, Solid State Commun. **70**, 153 (1989).

[15]K. Nakamoto, *Infrared and Raman Spectra of Inorganic and Coordination Compounds* (Wiley, New York, 1986), p. 130.

[16]E. T. Heyen, J. Kircher, and M. Cardona, Phys. Rev. B **45**, 3037 (1992).